

Automated condition assessment of concrete bridges with digital imaging

Ram S. Adhikari^a, Ashutosh Bagchi* and Osama Moselhi^b

Department of Building, Civil, and Environment Engineering, Concordia University, Montreal, Canada

(Received December 11, 2013, Revised April 20, 2014, Accepted April 25, 2014)

Abstract. The reliability of a Bridge management System depends on the quality of visual inspection and the reliable estimation of bridge condition rating. However, the current practices of visual inspection have been identified with several limitations, such as: they are time-consuming, provide incomplete information, and their reliance on inspectors' experience. To overcome such limitations, this paper presents an approach of automating the prediction of condition rating for bridges based on digital image analysis. The proposed methodology encompasses image acquisition, development of 3D visualization model, image processing, and condition rating model. Under this method, scaling defect in concrete bridge components is considered as a candidate defect and the guidelines in the Ontario Structure Inspection Manual (OSIM) have been adopted for developing and testing the proposed method. The automated algorithms for scaling depth prediction and mapping of condition ratings are based on training of back propagation neural networks. The result of developed models showed better prediction capability of condition rating over the existing methods such as, Naïve Bayes Classifiers and Bagged Decision Tree.

Keywords: visual inspection; 3D visualization model; condition rating; neural networks; image analysis; depth perception; bridge defects

1. Introduction

Civil infrastructure systems around the world are deteriorating at an alarming rate because of increased traffic, aging, environmental changes, radiation, and structural damages. The 2013 report card for America's Infrastructures reveals that the average age of 607,380 American bridges is 42 years; and about 11% of them are rated as structurally deficient (ASCE 2013). In Canada, more than 40% of the bridges currently in use were built over 50 years ago and are in need of immediate upgrade (Bisby and Briglio 2004). To ensure effective management of civil infrastructure, it is necessary to identify the critical structures, and evaluate their performance in order to verify that previously designed structures still satisfy the current code requirements. In general, the performance of a bridge is evaluated using two approaches. The first approach is based on reliability analysis of bridge structures considering the load and resistance models of infrastructures (Frangopol *et al.* 2008a, b, Ghodoosi *et al.* 2013). In recent years, the tracking of

*Corresponding author, Associate Professor, E-mail: ashutosh.bagchi@concordia.ca

^a Ph. D. Student, Email: ram_adhikari91@yahoo.com

^b Professor, Email: moselhi@encs.concordia.ca

real time performance of structures has been made possible by Structural Health Monitoring (SHM) systems using several types of sensors installed either on the surface or embedded inside bridge components (Humar *et al.* 2006, Lee *et al.* 2007, Bagchi *et al.* 2010). However, the application of SHM using various sensors can be expensive as compared to visual inspection (Orcesi and Frangopol (2010). On the other hand, the second approach of bridge performance evaluation is based on visual inspection which is one of the widely accepted methods adopted by government, as well as, by private agencies (AASHTO 2001, FHWA 2004). However, the performance evaluation based on visual inspections possesses several limitations, including them being time-consuming, providing incomplete information, and reliance on inspectors' experience (Moore *et al.* 2001).

In order to enhance the reliability of visual inspection, several non-destructive tests based on remote sensing technologies have been studied in the literature (Yehia *et al.* 2007). A systematic study by Ahlborn *et al.* (2010) on the condition assessment of concrete bridge decks demonstrated that the three dimensional optical bridge evaluation techniques, the bridge viewer remote camera system, and the GigaPan techniques based on Street View-style photography are the best technologies for defect measurement during bridge inspections. In their work, Agisoft Photo Scan, which is a close range 3D photogrammetric commercial software program, was used to develop 3D models with minimal digital photographic input. To ensure 60% overlap of photographs as required for image stitching, a truck was driven over the bridge deck at a speed of 1 mile per hour. Recently, Hinzen (2013) demonstrated that a systematic comparison of building damage evaluation is possible with Google street view data. The study showed that the Google street view resolution was sufficient to detect structural components damage, as well as defects like a crack as reported by the author. The above research shows the importance of digital image processing application for condition assessment of civil infrastructure. However, the application of digital image processing for automatic prediction of condition rating of structural components has not been studied earlier.

Abudayyeh *et al.* (2004) developed an imaging data model for automation of bridge monitoring and inspection. The developed model was integrated with PONTIS to enhance the reliability of visual inspection. Although the imaging data model demonstrated the capability of producing inspection reports automatically based on the stored information, the process of assigning condition rating for the structural components was done manually by experts. The current paper proposes a scheme for automated prediction of condition rating for bridge elements using artificial neural networks based on digital image processing. To illustrate the process, scaling defect of concrete structures is considered here as a candidate defect. The guidelines for assigning condition rating are based on Ontario Structure Inspection Manual (OSIM 2008). However, other inspection guidelines can also be used in this process.

2. Background

In current practices, bridge conditions are mainly assessed by bridge inspectors through their visual observations of defects occurred on bridge components, such as columns, girders, and decks (Zhu *et al.* 2010). As discussed in the previous section, the reliability of the visual inspection method has been questioned in the literature, and several measures have been suggested to enhance it (Moore *et al.* 2001). For example, visual inspections are time-consuming, and observational results are heavily dependent on inspectors' personal experiences (FHWA1991). In order to

overcome such limitations, several attempts have been made to automate visual inspection using computer vision techniques. One of such attempts is to automatically retrieve the three dimensional (3D) as-built/as-is bridge information, as well as quantification of defects using remote sensing techniques (Ahlborn *et al.* 2010, Zhu *et al.* 2010, and Adhikari *et al.* 2014). However, the application of digital image processing for developing defect quantification and 3D visualization models has several practical challenges.

The application of remote sensing in civil engineering can be defined as deriving information about the characteristics of civil infrastructure without being in contact with them (Aronoff 2005). Although, image-based remote sensing can be carried out using any part of the light spectrum, the common form of light bands used for imaging of civil infrastructure includes visible and infrared light bands. The digital photography is limited to visible light bands occupying a small portion of light spectrum varying from 400 nanometers (nm) to 700 nm (Ahlborn *et al.* 2010). For detection and quantification of bridge defects, a number of remote sensing technologies need to be integrated. The commonly used non-destructive techniques for condition evaluation of concrete decks are visual inspection, liquid penetrant dye, chain drag, Half-cell potential, acoustic emission, ultrasonic pulse velocity, ground penetrating radar, impact echo, and IR thermography (Yehia *et al.* 2007). Ground penetrating radar, impact echo, and IR thermography are found to be promising techniques for detection of internal defects in concrete bridge decks, while others could be suitable for detecting surface defects. Ahlborn *et al.* (2010) compared several remote sensing technologies for condition assessment of concrete bridge decks such as three dimensional optical bridge evaluation techniques, bridge viewer remote camera system, GigaPan, LIDAR, Thermal IR, Digital Image Correlation, Ground Penetrating radar, Remote Acoustics, and high resolution Street View-style digital photography. The study concluded that digital image based technologies are most suitable for quantification of defects because high resolution images of defects are possible to acquire using modern digital cameras. In a similar study, Hinzen (2013) demonstrated that a systematic comparison of building damage evaluation is possible with Google street view data. The study showed that the Google street view resolution was enough to detect structural components damage, as well as defects like a crack as reported by the author.

Although the 3D as-built/as-is bridge information is useful, the retrieval of such information is quite challenging (Remondino and El-Hakim 2006). McRobbie *et al.* (2010) discussed the importance of 3D visualization model for automated process of condition assessment of bridge structures which can mimic the on-site visual inspection of civil infrastructure. They investigated several off-the-shelf 3D software tools, such as MeshLab, Rhino, True Space, and Phtosynth, and found that the existing tools could not fully support the automatic retrieval of 3D as-built/as-is bridge information. In the process of developing a 3D model, a lot of manual editing and correction works are required, which makes the overall information retrieval process labour-intensive and time-consuming (Zhu 2012). So far, the methods for the retrieval of 3D bridge information are broadly classified into two groups. The methods in the first group were built upon the 3D point clouds captured directly by terrestrial laser scanners. The laser Scanners could collect millions of 3D points with one scan in minutes, but they are typically heavy and not portable (Foltz 2000). In addition, the 3D points collected by the laser scanner only record the spatial information of the bridges. As a contrast, the methods in the second group relied on the digital images or videos taken by digital cameras or camcorders. The digital cameras or camcorders are easy to use and portable, but the 3D information has to be obtained indirectly from multiple images or video frame shots taken from different directions. Both groups of methods have pros and cons in sensing accuracy, resolution, cost, etc. (Zhu *et al.* 2010). For such reasons,

researchers have been investigating the possibility of integrating the point clouds and digital images to enhance the current information retrieval process (El-Omari and Moselhi 2008, Zhu 2012). The importance of a 3D model also has been demonstrated by Hinzen *et al.* (2013) for comparing old excavation photographs with the currently obtained photographs in an archaeo-seismological study. For automatic integration of 3D point clouds and digital images, a preliminary study of 3D visualization model has been proposed for automatic condition assessment of civil structures (Adhikari *et al.* 2013).

2.1 Current trends in 3D visualization and their limitations

The Google Street view provides a continuous 360° viewing environment for civil infrastructure. Recently, Hinzen (2013) has demonstrated the feasibility of damage detection and quantification based on Google Street View images. However, since the technology uses the instrumentation mounted on a vehicle which moves along a bridge, this approach may not be suitable for condition assessment for elements lying underside of the bridge.

Since the imaging model is based on remote sensing technology, there is less disruption of traffic. By developing a technology which can be fixed with traffic moving at the same highway speed will maximize the benefit of such techniques. Digital image-based analysis of condition assessment of infrastructure provides low capital cost, rapid deployment, and useful metrics for the condition states (e.g., to compare condition at different instances of time, percentage area, volume, crack density, roughness index etc.). However, when the speed of data collection is low, there may be traffic disruption, and in that case, the requirement of high resolution images, field of view, and data processing time are the challenges that need to be improved further (Ahlborn *et al.* 2010, Hinzen 2013).

It is unlikely that fine cracks can be detected with the available resolution in the Google Street View. However, the detection accuracy of cracks can be increased using high resolution digital cameras. Currently, there is not enough literature available on detection of fine cracks using such technology. The resolution available in Google Street view images is useful for condition evaluation of bridge deck surface considering spalling and scaling, map visible cracks, joint damage, and delaminations (Ahlborn *et al.* 2010).

In order to improve the reliability of visual inspection, the developed methodology based on digital images needs to be integrated with existing bridge management system which is another challenge to be considered in developing an effective imaging model. In terms of cost, LiDAR scanners are the most expensive system for data acquisition and processing because they require digital camera, scanners, positioning system, computers, and software. Similarly, the data collection by digital cameras is much cheaper than GPR system (Ahlborn *et al.* 2010). Since each of the image based technologies has its own advantages and disadvantages, a proper combination of such technologies is required to provide better results.

Often, the size of defect measured from its digital image is expressed in pixels, which needs to be converted to conventional units such as feet or millimeter. Several authors have used either artificial or natural scales in the image frame for obtaining the physical size of damage from a digital image (Ahlborn *et al.* 2010, Adhikari *et al.* 2014). While working with digital images, the following criteria need to be considered: a) color; b) the distance between camera and object which is called field of view shall be such that the minimum resolution in 1 pixel per mm; and c) lighting should be uniform to maintain images are consistent, and images shall be overlapped to ensure full coverage (McRobbie *et al.* 2008). Apart from the general conditions, they suggested that for

improve accuracy and avoidance of parallax and projection errors, an image of a defect should be acquired from an orthogonal line of view to the plane on which the defect lies (McRobbie *et al.* 2008).

2.2 Neural networks for mapping of condition rating

Artificial neural networks (ANNs) are used for several purposes for developing data fitting regression models, as well as to solve classification problems where direct relations among input parameters do not exist. ANNs mimic the thought process of human brain by assigning weights to individual inputs attributes and output is mapped through a simple transfer functions (Liu 2001). Neural networks were used for automatic defects classification in sewer pipelines where digital images of sewer defects were used for extraction of geometric parameters (Moselhi and Shehab-Eldeen 2000), and the accuracy of their algorithm was reported to be 98.2%. In construction sites, neural networks were used to classify different objects segmented from video images for automated object identification (Chi and Caldas 2011). Khan *et al.* (2010) also used neural networks to analyze structural behavior of sewer pipes in terms of variation of condition ratings. The reported success rate of the developed model was 92.3%. The content based methodology was suggested for automatic identification of shapes, objects and materials assisting in construction and maintenance of projects (Brilakis *et al.* 2006, Ye *et al.* 2013). Also, decision processes regarding future conditions of an infrastructure depend on many variables. Such uncertainties in defects classification in sewer pipes were discussed using neuro-fuzzy networks (Sinha *et al.* 2003).

One of the most relevant applications of neural networks was developed for predicting the fatigue life and failure of reinforcing bars in concrete elements. Abdalla and Hawileh (2013) tested 15 specimens to measure fatigue failure of reinforcing bars and then neural networks were trained to predict failure patterns for the chosen samples. Also, researchers have used genetic algorithms for optimizing the solutions for structural design of bridge components (Krishnamoorthy 1999).

The temporal change in the condition state of a bridge element is affected by the uncertainties in many key parameters, which presents a significant challenge in effective decision making process. Liu (2010) studied 69 collapsed bridges in the U.S. built after 1967 and he found that more than 50% bridges collapsed due to collisions and natural disasters. Such phenomena are difficult to capture and incorporate into BMS to enhance the decision making process. Additionally, BMS do not consider environmental and geographical factors, material prices, and other design parameters which may lead to faulty prediction of bridge condition states (Liu and Frangopol 2006). Such problems to some extent can be addressed by revising the inspection frequency based on a risk-based management strategy. However, bridge inspections are time consuming and costly. Thus increasing the inspection frequency would increase the operation costs leading to unacceptable methodology for assigning condition rating. Therefore, the development of an automated bridge inspection system using computer vision approach is of interest as such methods can potentially track the damage propagation due to unknown events with less cost and time, allowing the feasibility of revising the inspection frequency. The preliminary work regarding to the automated prediction of condition rating based on digital image processing has been briefly demonstrated in Adhikari *et al.* (2012).

3. Methodology

The methodology encompasses data acquisition, 3D visualization model, image pre-processing, feature extraction, and development of neural networks for automated prediction of condition rating for structural elements as shown in Fig. 1. The 3D visualization model has been developed here based on digital images collected from a set of flexural tests on reinforced concrete beams in the structural engineering laboratory at Concordia University at Montreal. The 3D model is developed by projecting current digital images so that the current condition assessment is possible just by visualizing the model on a computer screen. Likewise, an automated procedure for prediction of condition rating requires feature extraction based on digital image processing. The procedure considers scaling defect as one of the surface defects in reinforced concrete structures and the mapping of condition rating based on OSIM (2008) guidelines is achieved through neural networks models. The condition rating according to the above guidelines are based on the severity of a scaling defect which depends on the depth of the defect. Therefore, before developing the neural networks models and training them, the depth of scaling defects must be identified. In the present work, the variation in RGB color profile is measured to quantify the depth perception and other geometric parameters are retrieved from the analysis of the digital images. The following paragraphs explain these aspects in details.

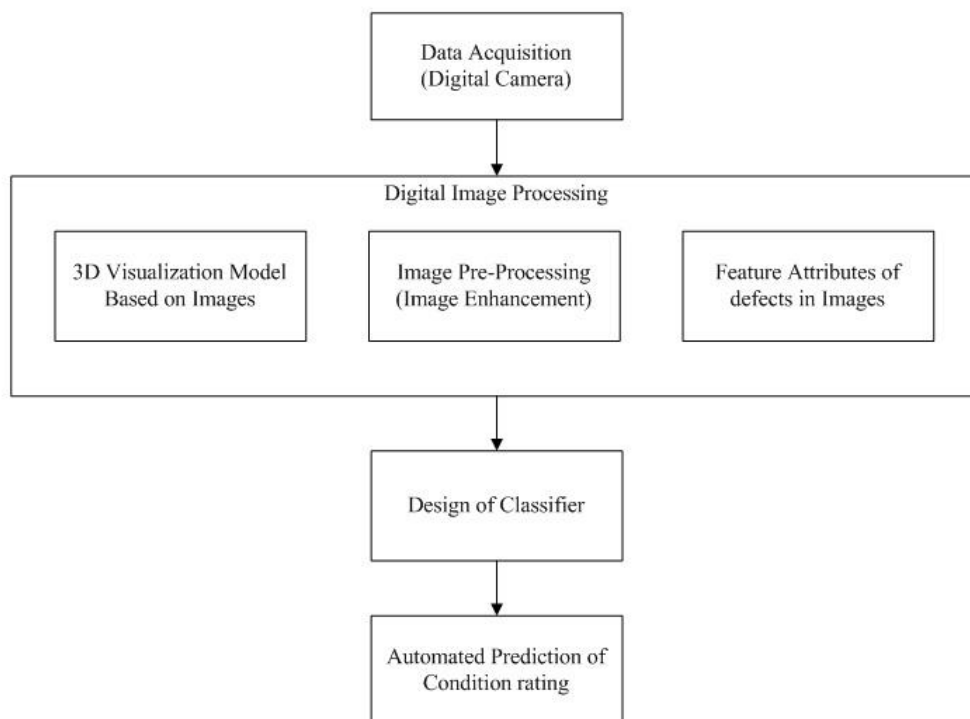


Fig. 1 Research methodology

3.1 Data acquisition

A commercially available digital camera (SONY) has been used here for acquiring the digital images of reinforced concrete surface defects. For the identification and quantification a defect, digital images are required to be taken at a close-range focusing on the details of the defect. Each photographic frame includes either natural or artificial targets for scaling purpose. Natural targets may include some structural details of the beams, columns, parapet walls and railings, patches on concrete and steel surfaces, and nuts or bolts on girders. When there are insufficient natural targets, artificial targets would be required to be placed in the vicinity of the area of interest (Jáuregui *et al.* 2006).

3.2 3D Visualization model

3D visualization model provides a good understanding of an object, and various features of the object can be derived from such models. This paper utilizes a direct method of image projection to generate 3D models with the help of the Google Sketch up software (2008). For a good better 3D, 4 images are required to be taken from each four corners of an object. However, a 3D model can also be developed just from a single image or two taken at 45° so that at least three corners are visible from a single position. Fig. 2 illustrates the four images considered for model development here, and Figs. 3 and 4 show the output of the model developed after projecting the actual image textures on the 3D model.



Fig. 2 (a) – (d) 2D images of Reinforced Concrete beams (for 3D model development)

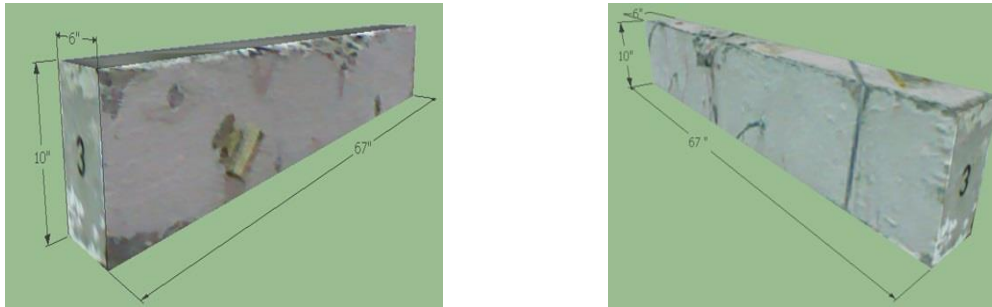


Fig. 3(a) – (b) 3D Visualization Model of a beam developed using digital images

3.3 Image pre-processing

Image pre-processing is one of the fundamental steps in image analysis which can be performed using spatial and frequency domain operations as summarized in Fig. 4 (Biswas 2008).

Spatial domain operation refers to direct manipulation of pixels in an image at local level or at global level (Xu *et al.* 2012 and Adhikari *et al.* 2012). On the other hand, frequency domain operation requires transforming digital images in frequency domain by Fourier Transform where the majority of information is contained at lower frequencies, while sharp information related to edges are retained with higher frequencies. Depending on situations, one can use high-pass or low-pass filter to enhance the image. In this paper, both spatial and frequency domains operations of image pre-processing have been used for image enhancement.

3.4 Imaging criteria's for data acquisition

A digital image is 2D projection of 3D real world objects. The effectiveness of digital image analysis highly depends upon the process how 3D to 2D projections occurs. The image projections can be broadly classified in two parts: perspective and orthographic projections (Solomon and Breckon 2011). Similarly, McRobbie (2008) showed that a single pixel in an image taken perpendicularly to a surface would represent a smaller area than the same pixel taken at an angle. Various imaging criteria were also listed in the above report; for example, the minimum pixel resolution should be 1 pixel/mm; camera position, elevation and bearing should be recorded while taking images; and successive images should be overlapped for image stitching problems. The orthography projection is defined mathematically by $x = m * X$ and $y = m * Y$, where m is a scaling factor which relates 3D real world coordinates given by (X, Y, Z) to the camera coordinates given by (x, y) . The projection is an affine transformation in which relative geometric relationship of objects are maintained. In practice, if we acquire images very close to the scene, it can be referred as orthographic projection, which is suitable for digital image analysis (Solomon and Breckon 2011).

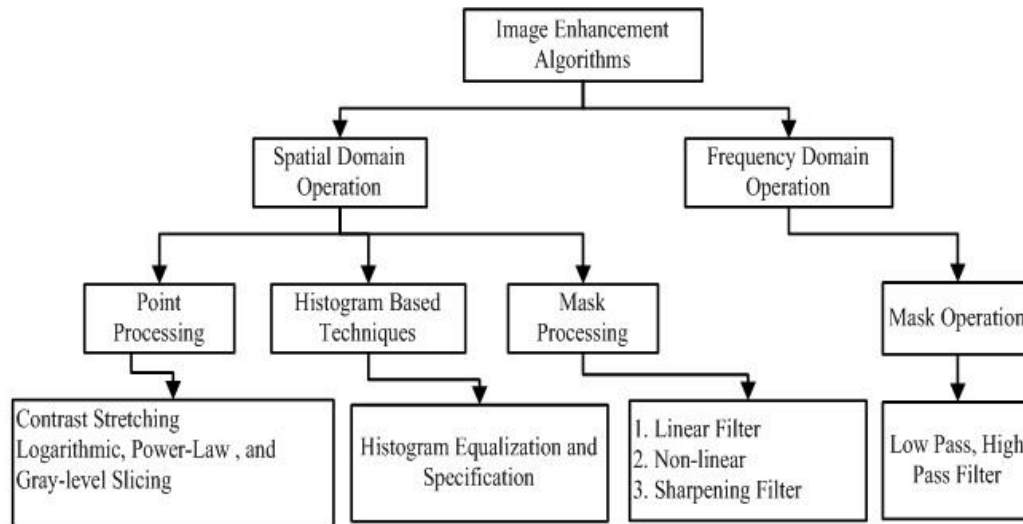


Fig. 4 Image Enhancement Techniques for Image Pre-processing

3.5 Artificial neural networks (ANN)

The neural networks are the ideal choice of algorithms when the solution cannot be represented by a flowchart (Heaton Research 2013). These algorithms do not have any restriction on their input data. The only underlying assumption in back propagation algorithm is that the input parameters shall not be changed during the forward and backward passes. In general, the solution of the problem is difficult to predict when it depends on various parameters and the final solution is highly dependent on the selected factors. The neural networks are ideal choice for prediction of condition rating for bridge condition assessment because bridge condition rating depends upon a number of parameters. Learning rate and momentum are the two important parameters which need to be selected carefully to develop an efficient and well trained neural network models.

While choosing multi-layer perceptron architectures, the number of neurons assigned to a layer is important. They are decided based on trial and error method. For the initial guess, one can use the number of neurons based on a thumb rule. For example, the number of neurons in a hidden layer may be taken as two third the size of input layers plus the size of output layers (Heaton Research 2013). Sometimes multi-layer perceptron and back propagation terms are used interchangeably. But, they have their own significance. Back propagation means propagation of errors in backward direction as shown in Fig. 5. Multi-layer perceptron has two types of signals. One is the functional signal which flows in the forward direction and the other is the error signal which flows in the backward direction.

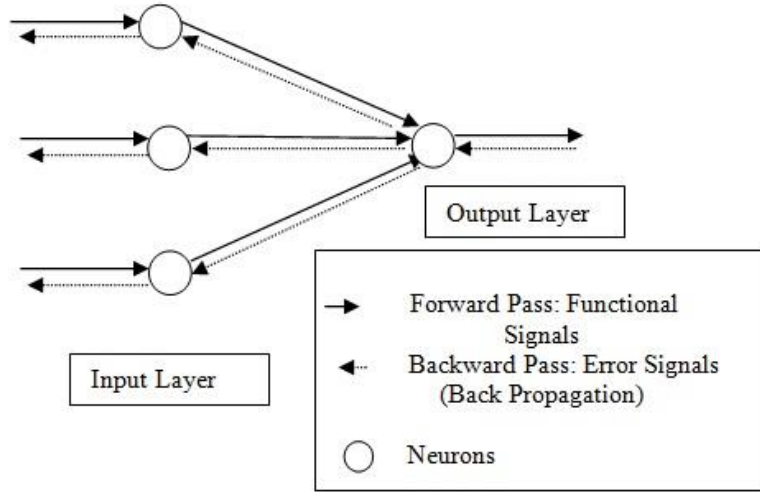


Fig. 5 Forward and backward pass for Back Propagation Algorithms

Back Propagation Algorithm:

At the n^{th} iteration (i.e. the presentation of n^{th} pattern in an epoch, where a complete set of patterns is called epoch), the error signal corresponding to a neuron j at the output layer is given by Eq. (1)

$$e_j(n) = d_j(n) - y_j(n) \quad (1)$$

where, d_j is the desired output of neuron j , and y_j is the actual output of neuron j . The change in synaptic weight $\Delta w_{ji}(n)$ can be estimated by Eq. (2)

$$\Delta w_{ji}(n) = \eta \delta_j(n) y_i(n) \quad (2)$$

where, η is the learning rate, y_i is the actual output in the previous layer, and $\delta_j(n)$ is the local gradient given by Eq. (3)

$$\delta_j(n) = -\frac{\partial E(n)}{\partial v_j(n)} \quad (3)$$

where, $\partial E(n)$ is the partial derivative of instantaneous error energy function, $E(n) = 1/2 \sum_j e_j^2(n)$; $\partial v_j(n)$ is the partial derivative of induced local field $v_j(n) = \sum_i^m w_{ji}(n) j_i(n)$, representing m as the number of neurons in the previous layers; and

$w_{ji}(n)$ is the synaptic weight. The only underlying problem in the Eq. (2) above is to calculate the local gradient. The problem can be divided into the following two cases.

Case 1: Neuron j belongs to output layer, in which case, $\delta_j(n)$ can be calculated from Eq. (3) because this is supervised learning and the output is known in advance.

Case 2: Neuron j belongs to a hidden layer. In this case, since the error in hidden layer is not known yet, it is difficult to determine $\delta_j(n)$. But, with the similar formulation as shown above, the local gradient in hidden layers can be estimated by using the Eq. (2) for weight adjustment.

4. Experiments and results

The proposed methodology for automated prediction of condition rating was implemented in MATLAB (Math works 2013), Google Sketch up (2008), and Neuroshell (Ward Systems 2013) in Windows Vista Enterprise 32 bit operating System. The desktop consists of Intel ® Core™ 2 Duo CPU, E6550 @ 2.33 GHz. A commercially available SONY-DSC T5 digital camera of 5.1 mega pixels with optical zoom 3X was used for image acquisition. Also, Image J, commercially available software (NIH, 2013) was used for extracting the digital information of an image and 3D visualizations.

4.1 Feature extraction

The proposed methodology requires high-resolution images to capture the concrete surface defects. To achieve high-resolution images, two cameras were used to collect images. The first camera photographs orthogonal images which are perpendicular to defect surfaces, while the second camera captures the whole concrete surface upon which defects lay. The use of hybrid camera for image acquisition was discussed in details by Nishimura *et al.* (2012). Various attributes considered for mapping of scaling depth and prediction of condition rating based on the severity of defects are listed in Fig. 6. In this paper, the attributes of a scaling defect are estimated by selecting a region of interest (ROI) as shown in Fig. 7(a).

The paper demonstrates the automated prediction of element condition rating for scaling defect only. Similar algorithms need to be developed for all types of concrete defects (e.g., spalling, cracking, exposed reinforcement, corrosion etc.) to fully automate the process of assigning condition rating based on digital images, which is not within the scope of this paper. 3D visualization model, which mimics the on-site visual inspection, is suitable for comparing structural conditions developed at different time periods. However, for defect quantification, the proposed research does not directly use the developed 3D visualization model, but it uses the same digital images used for developing a 3D model. The reason is that 2D images are already simplified and projected image of real 3D objects. 3D model development requires the projection of 2D images on 3D model to get current textures appearance. In such cases, many image processing algorithms yield poor results. For such reasons, the proposed methodology utilizes the original digital images for defect quantification purpose using digital image processing techniques. For such approach, a robust database management is necessary for handling the digital images.

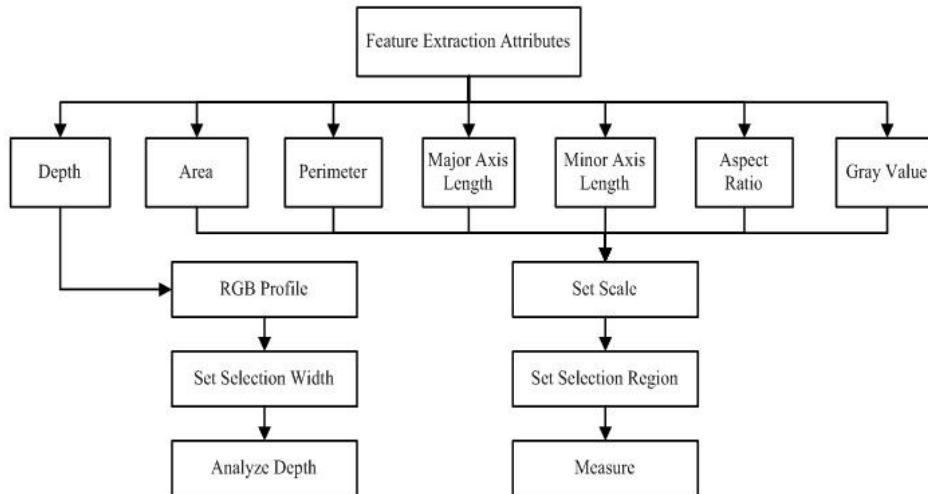


Fig. 6 Image Based Feature Extraction for scaling concrete defects

Also, it was realised that image acquisition methodology required for 3D model development and for defect quantification are different. For a better performance, oblique images (usually taken at 45° from a corner of a structure) are most appropriate for developing 3D models, whereas, for the defect quantification, orthogonal images are required for accurate results (usually taken perpendicular to the defect surface). The error occurred due to camera orientations for the same scene has been discussed in detail in Adhikari *et al.* (2014). For scaling defects, the feature extraction adopted for this research has been explained here.

The perception of distance based on light intensity was first discovered by Leonardo Da Vinci saying that “among bodies equal in size and distance, that which shines the more brightly seems to the eye nearer” (MacCurdy 1938). After that a number of studies were done to validate the hypothesis concerning the intensity of light and object distance relationship (Samonds *et al.* 2012, Coules 1955 and Ashley 1898). This paper adopts the clue of intensity variation of light with depth as shown in Figs. 7(a)-7(c). It is evident from the 3D visualization of color profile that brighter the intensity the lower depth perception. However, obtaining a numerical value of depth in accordance to the variation in the light intensity is not straightforward. In the present work, the sectional RGB color profile at the line of interest was used for quantifying the depth perception. The RGB profile obtained with line width of 1 unit is noisy. To filter such noise, the width of the line (selection region) has been increased to 30 units leading to smooth intensity variation with pixels distance in mm as shown in Fig. 8.

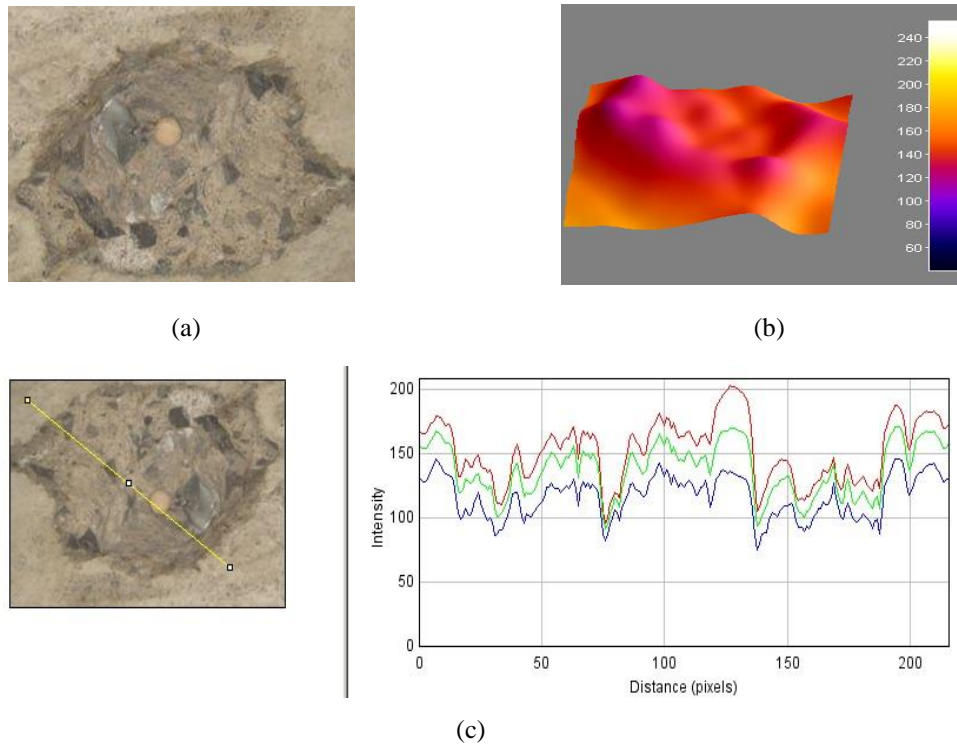


Fig. 7 (a) Region of Interests with scaling defects (b) 3D Visualization of Scaling Defects and (c) (1-2) Red, Green, and Blue Color Profile (Rough Intensity Variation along Section)

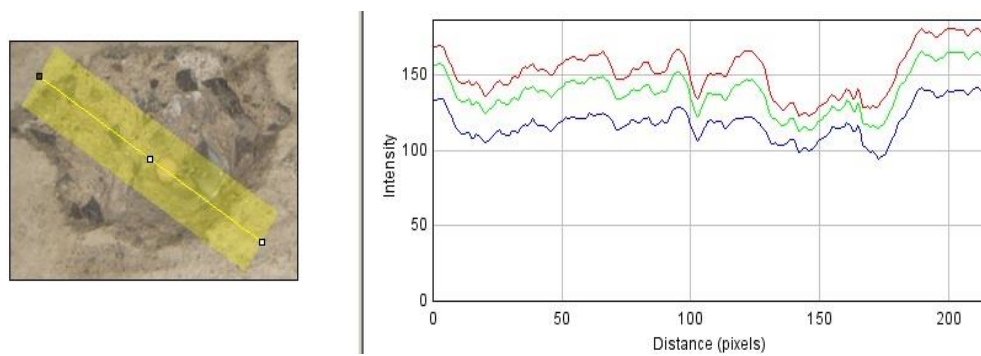


Fig. 8 (a)- (b) Red, Green, and Blue Color Profile (Smooth Intensity Variation along Section)

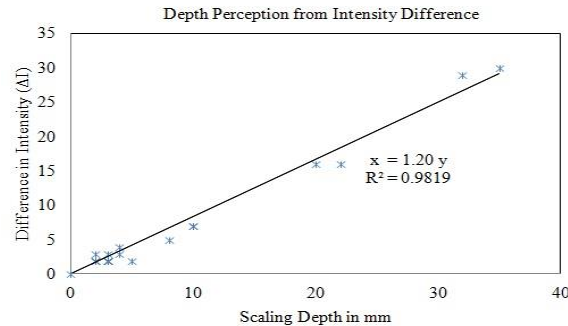


Fig. 9 Scaling Depth Estimation from Red, Green, and Blue Color Profile

The data are plotted in order to establish a relationship between light intensity (ΔI) based on RGB sectional color profile of an image. Now, the difference in intensity needs to be correlated to the real depth in engineering units. For this purpose, the depth of individual real scaling defect is measured using measuring scales and a straight line is fitted between the difference in intensity and depth as shown in Fig. 9. It was found that for the selected images, the difference in intensity showed a maximum of 20% error in depth estimation.

4.2 Check for normal distribution

Seven input parameters were retrieved from the selected digital images shown in Fig. 6. The simplest model for such mapping problem is to use the discriminant analysis. However, the discriminant analysis requires the data to be normally distributed. But, the plot of data set as shown in Fig. 10 clearly shows that data sets deviate from the red lines (i.e., normal distribution) indicating that they are not normally distributed. So, the discriminant analysis for such problems does not seem to be an appropriate choice; and hence, neural networks are chosen for mapping of the condition rating, which is explained in the next section.

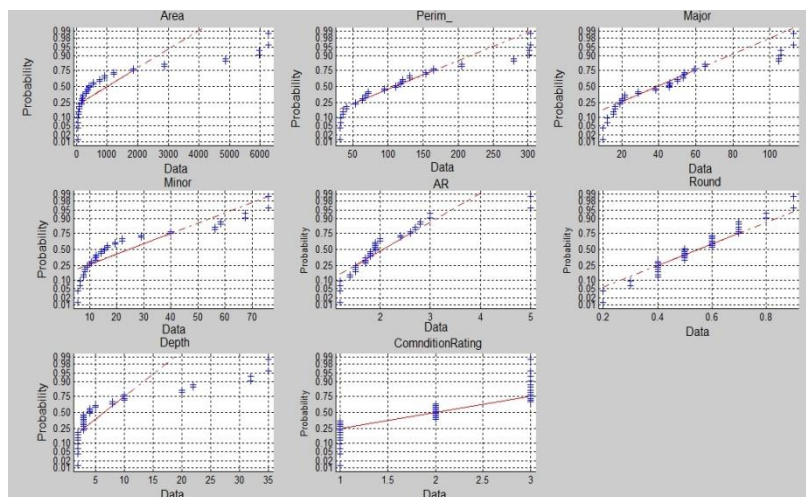


Fig. 10 Plot of Scaling Defects Feature Attributes to check for Normal Distribution of input parameters

4.3 Back Propagation Neural Networks (BPNN) Models

The training of BPNN model is based on supervised learning. The relationship between the depth and condition rating of structural elements has been represented by a back propagation neural network. The following two models were constructed: Model 'a' to predict the scaling depth, and Model 'b' to predict the condition rating as shown in Fig. 11. Model 'b' contains depth as an additional input variable in the data pattern to predict the condition state (CS) rating for bridge elements based on the severity of observed defects in comparison to Model 'a'.

The guidelines provided in the Ontario Structure Inspection Manual (OSIM 2008) were used for determining the Condition Rating of a concrete bridge element. Table 1 summarizes the condition state rating grades as suggested in OSIM (2008). The condition state rating of 1 indicates a light level of scaling damage and 3 indicates a severe level of scaling damage. The input data used in the BPNN models were normalized (between 0 and 1) using the Eq. (4).

$$X_{ni} = (X_i - X_{min}) / (X_{max} - X_{min}) \quad (4)$$

where, X_{ni} is the normalized value of X_i ; X_i is the i^{th} value of a data series with X representing the raw data; X_{min} is the minimum value of X in the sample set; and X_{max} is the maximum value of X in the sample set.

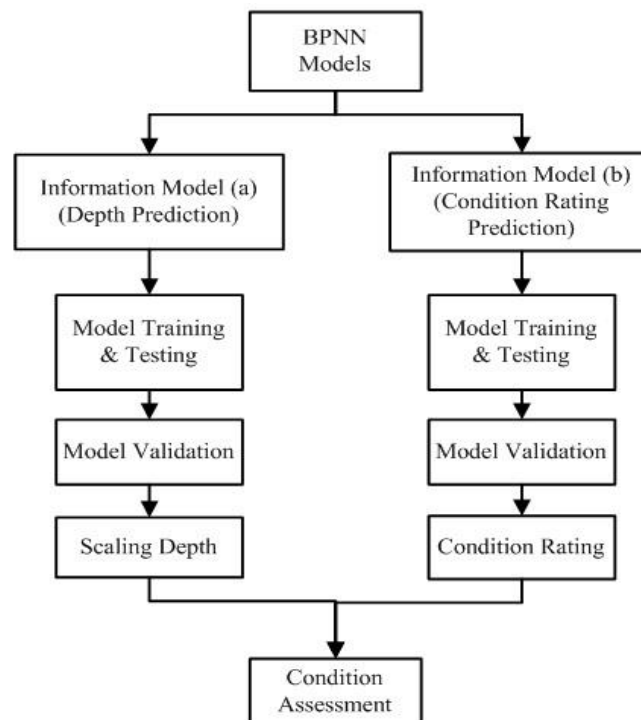


Fig. 11 Back propagation Neural networks Models

Table1 Description of Condition Rating based on OSIM (2008) guidelines for Scaling Defects

Defects	Condition State Rating		
	Light (1)	Medium (2)	Severe (3)
Scaling	Local Flaking/Loss of Surface Portion of Concrete or Mortar due to Freeze or Thaw		
	Up to 5 mm Depth	6-10 mm Depth	> 10 mm Depth

4.4 Training of the BPNN

The model architecture is shown in Table 2 and the training process of the neural networks is explained in Fig. 12. The detailed information on the layers, number of neurons, and the adopted activation functions are also listed in Table 2. The architecture of the network consisted of five layers of neurons with one input layer (the number of input neurons are equal to number of attributes in each pattern), 3 hidden layers, and one output layer (the number of output neuron is one). A total of 19 data patterns are extracted from the selected images from real bridges using the image analysis which consisted of 60% data for training sets, 20% data testing sets, and 20% data for validation sets. The validation data sets are also called the production set. The production set of data, which is not presented to the network during training, is later used to validate the model.

The learning rate, momentum, and initial synaptic weight during the initial training process have been assigned 0.2, 0.2, and 0.3 respectively. The initial choices of this parameter have impact on performance of the designed model. Appropriate the initial values for these parameters are very important for constructing a successful and efficient model. The Stopping criteria of these networks are explained in next paragraphs.

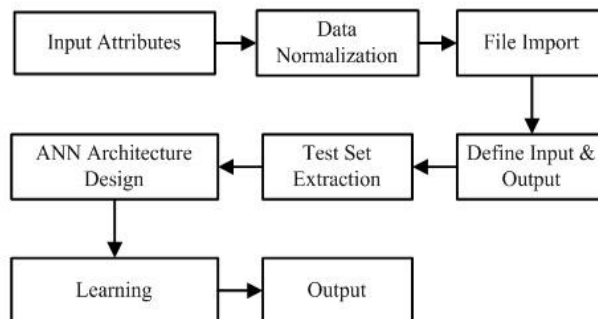


Fig. 12 Neural Network Models Work Flow Diagram

Table 2 Neural Networks Design and Stopping Criteria

Slab Number	Number of Neurons	Activation Functions	Learning Rate	Momentum	Initial Weight
1	7	Linear (0,1)	0.1	0.1	0.3
2	2	Gaussian	0.1	0.1	0.3
3	2	Tanh	0.1	0.1	0.3
4	3	Gaussian comp	0.1	0.1	0.3
5	1	Logistic	0.1	0.1	0.3
Training					
Stop training when one of these is true about the training set			Average error <	0.0002	
			Epochs since minimum average error >		1,000
			Calibration interval (events)		200
Stop training when one of these is true about the test set			Events since minimum average error >	20,000	

Table 3 (a) Performance of Depth Prediction Model and (b) Performance of Condition Rating Prediction Model

Patterns processed	19	Patterns processed	19
R squared	0.7024	R squared	0.9807
r squared	.7990	r squared	0.9839
Mean squared error	0.028	Mean squared error	0.003
Mean absolute error	0.147	Mean absolute error	0.032
Min. absolute error	0	Min. absolute error	0.000
Max. Absolute error	0.278	Max. Absolute error	0.167
Correlation coefficient r	0.8939	Correlation coefficient r	0.9919
(a)		(b)	

After the model is developed as discussed above, the input patterns can be presented to the network either in a rotational or a random order at every epoch. It is observed that the random training patterns work better and adopted for the training of entire network. Also, the network's weight is updated through momentum option which utilizes a portion of the previous weight change for the network. The adopted process stabilizes the direction of the training and produces acceptable results as presented in subsequent Tables.

Table 4 (a) Contribution factors for Depth Prediction Model and (b) Contribution factors for Condition rating prediction

Ranking	Parameter	CF	Ranking	Parameter	CF
1	Length of Major Axis	27.6%	1	Depth	53%
2	Area	23.8%	2	Length of Minor Axis	9.6%
3	Length of Minor Axis	19.6%	3	Aspect Ratio	8.8%
4	Aspect Ratio	12.2%	4	Roundness	7.6%
5	Perimeter	9.9%	5	Length of Major Axis	7.2%
6	Roundness	6.7%	6	Perimeter	6.8%
			7	Area	6.7%

(a)
(b)

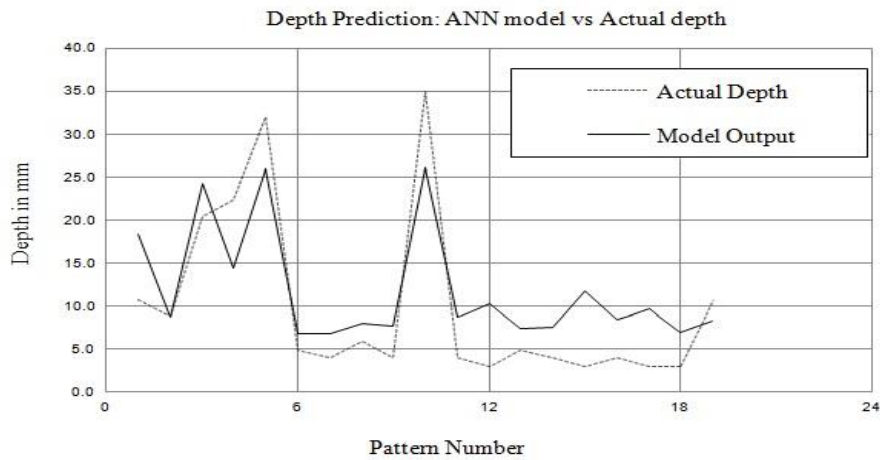


Fig. 13 Scaling Depth Prediction (Actual DepthVs Model Output)

The accuracy of the developed models is evaluated by applying the validation sets of data to the models. The validation sets of data are not exposed to the models during the training and testing phases. After training the developed models, various statistical parameters are obtained to measure the accuracy of the output variable. The developed BPNN model for depth prediction shows the accuracy of 89% as shown in Table 3(a), whereas the BPNN model for the estimation of the condition rating shows the accuracy of 99% as shown in Table 3(b), in terms of the corresponding correlation coefficient (CF).

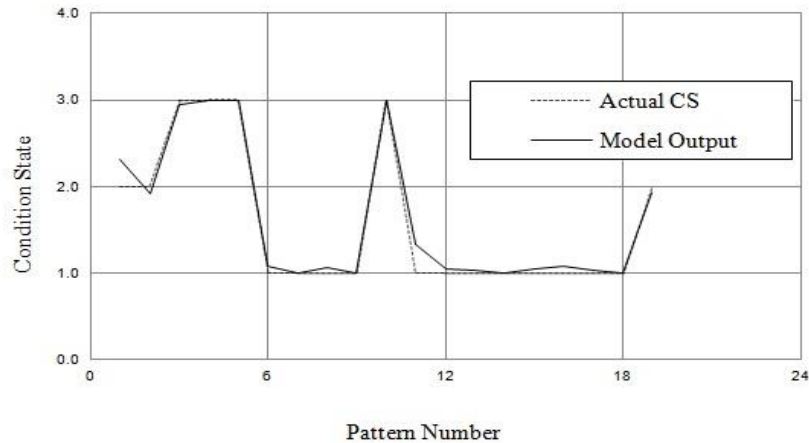


Fig. 14 Predicted Condition Ratings (Actual Condition Rating Vs Model Output)

Likewise, Table 4 shows how each of the input variables contributes to the decision making process of a network using back propagation algorithm. A low contribution from a variable does not mean that it is unimportant and can be removed from the inputs. Since the training of the network is based on overall patterns instead of individual variables, a variable with small contribution may be critical in some cases. From Table 4, it is observed that depth has the largest contribution, in predicting condition rating, which is 53%; whereas, surface area has the lowest contribution of 6.7%. The results are also expressed in graphical way by plotting the model output against the actual output as shown in Figs. 13 and 14 for scaling depth and condition rating, respectively. The graphs show the predicted values by the developed models and the actual values matched well indicating that the models can be used to solve for future problems reliably.

4.5 Comparison with other classifiers

4.5.1 Naïve bayes classifier

Bayes' rule is given by Eq. (5),

$$P(H/E) = \frac{P(E/H) \times P(H)}{P(E)} \quad (5)$$

The basic idea of Bayes's theorem is that the probability of an event (H) can be predicted based on some evidences (E). A prior probability of H or $P(H)$ is the probability of an event before the evidence is observed. A posterior probability of H or $P(H|E)$ is the probability of an event after the evidence is observed. It classifies data in two steps:

- **Training Steps:** The method determines the probability distribution based on the training sample assuming that the feature is conditionally independent for the given class.
- **Prediction Steps:** The method calculates the posterior probability of the data set which is unseen to the model; and then classifies the test sample based on the largest posterior probability.

The independence of the data sets is an underlined assumption for Naïve Bayes Classifier. To check the accuracy of the Naïve Bayes Model, Bayes Error is calculated using statistical tools and was found as 66%. The Bayes error shows that only 34% of the test data sets are correctly classified and 66% of test set data are wrongly classified. The analysis is tested for the importance of each parameter and the process indicated that only two input parameters “Major Axis Length” and “Depth” are important for this problem. This shows that the model with many input parameters may not always produce better results because this kind of model might have problem of data over-fitting.

4.5.2 Bagged decision tree model

Bagged Decision Tree is another type of machine learning algorithm which can improve the classification accuracy and stability of the training process. It reduces variance and avoids data over fitting problems. This method has better capability than Naïve Bayes Classifier and it can also measure the feature importance of input parameters. The bagged decision tree algorithm is performed on the previous data set and out of bag error was found as 37% which showed better accuracy than Naïve Bayes Classifier which has 66% error. Also, the importance factors for the input parameter were calculated as shown in Fig. 15. It showed that feature number 5 (Aspect ratio) and 6 (Roundness) did not contribute significantly to classification problem. The highest contributing factor for this classification is depth, which has a contribution of more than 65%.

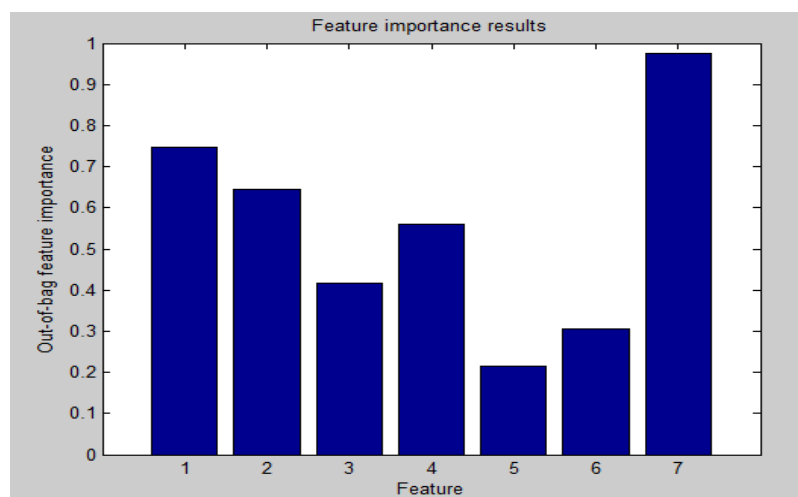


Fig. 15 Defects Feature Importance factors (Out of Bag algorithms)

Table 5 Comparison of results from different classifiers

Classifiers	Naïve Bayes Classifier	Bagged Decision Tree	Artificial neural networks
Accurately Predicted	34%	63%	99%

Table 5 summarizes the results of different classifiers. The results show that the prediction capability of neural networks was better than other classifiers showing 99% of predicting accuracy. The Naïve Bayes Classifier showed only 34% of data was classified correctly, whereas Bagged Decision tree was able to correctly classify 63% of input data. The neural networks did not have any underlying assumptions on the requirements in input data during training process except that during a complete cycle of back propagation (forward pass and backward pass), the input data patterns should not be changed. For other classifiers, there are fundamental assumptions associated with specific requirements in input data which might be the reasons of the inaccuracies. The accuracy of the developed NN models was evaluated by applying the validation data sets which were set aside before starting the training procedures. After applying these sets of data, various statistical parameters were obtained to measure the accuracy of prediction of condition state ratings. The statistical features of the trained BPNN models are shown in Tables 3 and 4.

5. Discussion and limitation of the developed models

Four different types of classification algorithms (i.e., linear discriminant analysis, artificial neural networks, Naïve Bayes Classifier, and Bagged Decision Tree Model) are presented here to determine the condition of concrete bridge elements with scaling defect, and the results of these methods have been compared to verify their effectiveness. The choice of an algorithm involves a tradeoff between the complexity of the algorithm and the assumptions made to simplify the problems in data manipulation. For example, the linear discriminant analysis is the simplest algorithm for classification; but it utilizes a restrictive assumption on the data. On the other hand, a complex algorithm like artificial neural networks operates over a wide variety of data sets, but the algorithms are more computationally intensive and difficult to work with. The current work considered only scaling defects for prediction of element condition ratings. However, an element might consist of several types of defects and each individual defect (extent and severity) contributes to the element's condition rating. Thus, for the proper condition assessment of elements, several expert functions need to be developed which can be integrated together to obtain a single condition rating for the element.

The depth perception of defects is highly influenced by lighting conditions. The mapping of difference in lighting intensity (ΔI) and defect depths work well when digital images are taken in similar lighting conditions. However, in actual practice it is difficult to maintain the same lighting conditions during image acquisition. So, this is one of the limitations of digital image processing, however, the error can be minimized through applying image pre-processing algorithms. The 3D visualization model for a concrete beam member is developed manually which needs to be automated using 3D point clouds. This is an important research topic in itself and the details are not discussed in this work. Further work is necessary to develop algorithms for processing 3D point cloud data to obtain the surface defect attributes, which is out of the scope of the present work. This paper demonstrates the methodology for estimating of condition rating for bridges

based on 19 data patterns obtained from analyzing digital images. However, the output of the models can be updated with additional information if available.

The defects quantification is performed based on original digital images instead of using the 3D visualization model for better accuracy. In absence of original images, the visualization model can also be used for defect quantification.

6. Conclusions

A condition state of a structural element represents the nature and extent of damages, whereas a condition rating of an element is derived by comparing the condition state of the bridge element with the as-built condition. However, the method of determining condition rating based on visual inspection has been reported to have several limitations; for example, the process is time consuming, subjective in nature, and often produces incomplete information. To overcome such limitations and improve the efficiency of BMSs, this paper presents a process to determine the condition ratings models based on digital image processing and neural networks, which can be potentially automated. The developed method is expected to augment the information provided in a visual inspection and contribute to improved decision making.

The proposed methodology considers scaling defects to demonstrate the proposed work in which condition ratings are mapped using digital image processing. The guidelines of the Ontario Structure Inspection Manual have been used for such mapping. The method requires the development of a quantification model for scaling defects (e.g., scaling depth estimation), image pre-processing, design of 3D visualization model for visual comparison of element condition states over different period of time, and condition rating model using computer vision approach. A 3D visualization is developed and presented for condition assessment of concrete bridges based on digital images acquired during flexural testing of reinforced concrete beams in the lab environment. Two BPNN models are developed here: the depth prediction model, and mapping of condition rating of concrete elements with scaling defects. A total of 19 data patterns have been prepared using the image analysis process which consisted of 60% data in the training sets, 20% data in the testing sets, and 20% data in the validation sets. The model contains 5 layers of neurons; one input layer, three hidden layers, and one output layer with several types of activation functions in each layer. The production data set, which has not been presented to the network during its training, is later used to validate the model. The statistical features of the trained BPNN models are measured in terms of prediction accuracy and contribution factors of input variables. Also, a comparison of the estimated depth output by the BPNN model and the actual one for all data points are plotted, and the acceptable accuracy has been observed showing a correlation coefficient of 89%. Similarly, the predicted condition ratings after training of the neural networks are plotted with the actual condition rating obtained according to the OSIM (2008) manual, and the accuracy of the prediction of condition rating has been observed 99% as a correlation coefficient.

The trained NN models work in a similar way as experts classify and predict the attributes of defects based on their experience. The procedure can potentially reduce the inspection time as inspectors need only to take engineering photographs, and analyze them using the proposed methods. Since the proposed method is fast and less expensive, it can be potentially used for rapid screening of deteriorating concrete bridges. In addition, the frequency of inspection can perhaps be altered to provide additional safety to bridges by recognizing the effect of extreme loadings and defect propagation. The research showed that 3D visualization bridge model can be used for

assigning element condition rating utilizing the digital images for assessing defects inflicted on bridge components. The developed models can also be merged with available automated trading systems or they can be integrated to excel for ranking of projects if inspection engineers do not have access to any BMS.

Acknowledgments

The authors would like to thank Concordia University, Montreal, Canada; and Natural Sciences and Engineering Research Council of Canada (NSERC) for financial supports for this research. The valuable comments and information about condition of bridges in Quebec provided by Mr. Adel Zaki, Chief Engineer (Roads and Bridges), SNC Lavalin Inc. are also gratefully acknowledged. The authors also wish to thanks to Mr. Arash Rahmatian, a PhD candidate at Concordia University, for providing digital images from a set of bending test of reinforced concrete beams. The contribution of all experts participated in this work is also gratefully acknowledged.

References

- AASHTO (2001), *American association of state and highway transportation officials*, Manual for condition evaluation of bridges, 2nd Ed., Washington, D.C
- Abdalla, J.A. and Hawileh, R.A. (2013), "Artificial neural network predictions of fatigue life of steel bars based on hysteretic energy", *J. Comput. Civil Eng.*, **27**(5), 489-496.
- Abudayyeh, O., Al Bataineh, M. and Abdel-Qader, I. (2004), "An imaging data model for concrete bridge inspection", *Adv. Eng. Softw.*, **35** (8-9), 473-480
- Adhikari, R.S., Moselhi, O. and Bagchi, A. (2012), "Automated prediction of condition state rating in bridge inspection", *Gerontechnology*, **11**(2), 81
- Adhikari, R.S., Moselhi, O. and Bagchi, A. (2014), "Image-based retrieval of concrete crack properties for bridge inspection", *Automat. Constr.*, **39**, 180-194.
- Adhikari, R.S., Zhu, Z., Moselhi, O. and Bagchi, A., (2013), "Automated bridge condition assessment with hybrid sensing", *Proceedings of the 30th International Symposium on Automation and Robotics in Construction (ISARC 2013)*, August 11 to 15, 2013 in Montreal, Canada.
- Ahlborn, T.M., Shuchman, R., Sutter, L.L., Brooks, C.N., Harris, D.K., Burns, J.W. and Oats, R.C. (2010), *An evaluation of commercially available remote sensors for assessing highway bridge condition*. Transportation Research Board.
- ASCE (2013), "Report card for America's infrastructure", <http://www.infrastructurereportcard.org/>, (Accessed October, 2013).
- Ashley M.L. (1898), "Concerning the significance of intensity of light in visual estimates of depth", *Psychol. Rev.*, **5**, 595-615.
- Aronoff, S. (2005), *Remote sensing for GIS managers*, Redlands, CA, ESRI Press.
- Bagchi, A., Humar, J., Xu, H. and Noman, A. (2010), "Model-based damage identification in a continuous bridge using vibration data", *J. Perform. Constr. Fac.*, **24**(2), 148-158.
- Bisby, L.A. and Briglio, M.B. (2004), ISIS Canada educational module No. 5: An introduction to structural health monitoring, ISIS Canada Research Network, University of Manitoba, Winnipeg, Canada, [http://www.isiscanada.com/education/Students/ISIS%20EC%20Module%205%20-%20Notes%20\(Students\).pdf](http://www.isiscanada.com/education/Students/ISIS%20EC%20Module%205%20-%20Notes%20(Students).pdf)

- Biswas, P.K. (2008), Online video lectures on digital image processing, NPTEL, IIT Kharagpur, Department of Electronics and Communication Engineering, <http://nptel.iitm.ac.in/syllabus/syllabus.php?subjectId=117105079>, (accessed October, 2013).
- Brilakis, I.K., Soibelman, L. and Shinagawa, Y. (2006), "Construction site image retrieval based on material cluster recognition", *Adv. Eng. Inform.*, **20**(4), 443-452.
- Chi, S. and Caldas, C.H. (2011), "Automated object identification using optical video cameras on construction sites", *Comput.Aided Civil Infrastr. Eng.*, **26**(5), 368-380.
- Coules, J. (1955), "Effect of photometric brightness on judgments of distance", *J. Exp Psychol.*, **50**, 19-25.
- El-Omari, S. and Moselhi, O. (2008), "Integrating 3D laser scanning and photogrammetry for progress measurement of construction work", *Automat. Constr.*, **18**(1), 1-9.
- FHWA (2004), "Federal Highway Administration (FHWA), National bridge inspection standards", *Federal Register*, **69** (239) 74419-74439.
- FHWA (1991), *Federal Highway Administration (FHWA)*, Bridge inspections training manual, July 1991.
- Foltz, B. (2000), "Application: 3D laser scanner provides benefits for Penn DOT bridge and rock face surveys", *Prof. Surv.*, **20**(5), 22-28.
- Frangopol, D.M., Strauss, A. and Kim, S. (2008a), "Bridge reliability assessment based on monitoring", *J. Bridge Eng.*, **13**(3), 258-270.
- Frangopol, D.M., Strauss, A. and Kim, S. (2008b), "Use of monitoring extreme data for the performance prediction of structures: General approach." *Eng. Struct.*, **30**(12), 3644-3653.
- Ghodoosi, F., Bagchi, A. and Zayed, T. (2013), *A deterioration model for concrete bridge deck using system reliability analysis*, Transportation Research Board (TRB) Conference, Washington, DC, January.
- Google sketch up (2008), 3D for everyone, <http://www.sketchup.com/intl/en/index.html>
- Heaton Research (2013), Online resources, introduction to neural networks using C#, <http://www.jeffheaton.com/ai/>, (accessed October, 2013).
- Hinzen, K.G. (2013), "Support of macroseismic documentation by data from Google Street View", *Seismol. Res. Lett.*, **84**(6), 982-990
- Hinzen, K.G., Fleischer, H. Hinojosa, J. Maran, U. Meinhardt, S.K. Reamer, G.S. and Tzislakis, J. (2013), "The mycenaean palace of tiryns, elements of a comprehensive archaeo seismic study", *Seismol. Res. Lett.*, **84**, 350.
- Humar, J., Bagchi, A. and Xu, H. (2006), "Performance analysis of vibration based techniques for structural damage identification", *Struct.Health Monit.*, **5**(3), 215-227.
- Jáuregui, D.V., Tian, Y. and Jiang, R. (2006), "Photogrammetry applications in routine bridge inspection and historic bridge documentation", *J. Transport. Res. Board*, **1958** (1), 24-32.
- Khan, Z., Zayed, T. and Moselhi, O. (2009), "Structural condition assessment of sewer pipe lines", *J. Perform. Constr. Fac.*, **24**(2), 170-179.
- Krishnamoorthy, C.S. (1999), "Structural optimization in practice: potential applications of genetic algorithms", *Struct. Eng. Mech.*, **11**(2), 151-70.
- Lee, J.J., Fukuda, Y., Shinozuka, M., Cho, S. and Yun, C. (2007), "Development and application of a vision-based displacement measurement system for structural health monitoring of civil structures", *Smart Struct. Syst.*, **3**(3), 373-384.
- Liu G.P. (2001), *"Neural networks" nonlinear identification and control: a neural network approach*, Springer, London.
- Liu, W. (2010), "Terrestrial LiDAR-based bridge evaluation", *Dissertation Abstracts Int.*, **71**(6).
- Liu M. and Frangopol, D.M. (2006), *Decision support system for bridge network maintenance planning*, In *Advances in Engineering Structures, Mechanics & Construction* (pp. 833-840), Springer Netherlands
- MacCurdy E. (1938), *The Notebooks of Leonardo Da Vinci volume I*, London: Jonathan Cape.
- Math works (2013), MATLAB Statistical Tool Box, Version R2012a, <http://www.mathworks.com/products/statistics/>, (accessed October, 2013).
- McRobbie, S. (2008), *PPR 338: Automated inspection of highway structures – Stage -3*, Crowthorne, Transportation Research Laboratory (TRL).

- McRobbie, S., Woodward, R. and Wright, A. (2010), *Visualisation and display of automated bridge inspection results*, Transport Research Laboratory, UK.
- Moore, M., Phares, B., Graybeal, B., Rolander, D. and Washer, G.A. (2001), *Reliability of visual inspection for highway bridges*, Volume I: Final report and, Volume II: Appendices, U.S. Department Of Transportation, Washington, D.C, 2001 FHWARD- 01- 0(021)
- Moselhi, O. and Shehab-Eldeen, T. (2000), "Classification of defects in sewer pipes using neural networks", *J. Infrastruct. Syst.*, **6**(3), 97-104.
- NIH (2013), Image J 1.45s, Commercial software for image analysis, online resources, National Institutes of Health, USA, <http://rsb.info.nih.gov/ij/>, (accessed October, 2013).
- Orcesi, A.D. and Frangopol, D.M. (2010b), "Use of lifetime functions in the optimization of non-destructive inspection strategies for bridges", *J. Struct. Eng. - ASCE*, **137**(4), 531-539.
- OSIM (2008), *Ontario structure inspection manual*, Ministry of Transportation, Engineering Standards Branch Bridge Office, Ontario, ISBN 0-7794-0431-9
- Remondino, F. and El-Hakim, S. (2006), "Image-based 3d modelling: a review", *Photogramm. Rec.*, **21**(115), 269-291.
- Nishimura, S., Kimoto, K., Kusuhara, S., Kawabata, S., Abe, A. and Okazawa, T. (2012), "Development of a hybrid camera system for bridge inspection", *Rammed Earth Conservation*, **440**.
- Samonds, J.M., Potetz, B.R. and Lee, T.S. (2012), "Relative luminance and binocular disparity preferences are correlated in macaque primary visual cortex, matching natural scene statistics", *Proc. National Academy Sci.*, **109**(16), 6313-6318.
- Sinha, S.K., Fieguth, P.W. and Polak, M.A. (2003), "Computer vision techniques for automatic structural assessment of underground pipes", *Comput. Aided Civil Infrastr. Eng.*, **18**(2), 95-112.
- Solomon, C. and Breckon, T. (2011), *Fundamentals of digital image processing: a practical approach with examples in matlab*, John Wiley & Sons.
- Ward Systems (2013), Neuroshell 2, Release 4, (1993-2000), Online Documentation. <http://www.wardsystems.com/manuals/neuroshell2/index.html?idxhowuse.htm>, (accessed October, 2013).
- Xu, G.B., Zhou, M.J, Xiong, Z.G. and Yin, Y.X. (2012), "An improved adaptive fusion edge detection Algorithm for road images", *AISS*, **4**(4), 129-137.
- Ye, X.W., Ni, Y.Q., Wai, T.T., Wong, K.Y., Zhang, X.M. and Xu, F. (2013), "A vision-based system for dynamic displacement measurement of long-span bridges: algorithm and verification", *Smart Struct. Syst.*, **12**(3), 363-379.
- Yehia, S., Abudayyeh, O., Nabulsi, S. and Abdelqader, I. (2007), "Detection of common defects in concrete bridge decks using non-destructive evaluation techniques", *J. Bridge Eng.*, **12**(2), 215-225.
- Zhu, Z. (2012), "Automated as-built modeling with spatial and visual data fusion", *Proceedings of the 12th International Conference on Construction Applications of Virtual Reality*, Nov. 1-2, Taipei, Taiwan.
- Zhu, Z., German, S. and Brilakis, I. (2010), "Detection of large-scale concrete columns for automated bridge inspection", *Automat. Constr.*, **19**(8) 1047-1055.